Membrane Helix Orientation from Linear Dichroism of Infrared Attenuated Total Reflection Spectra

Burkhard Bechinger,* Jean-Marie Ruysschaert,# and Erik Goormaghtigh#
*Max-Planck-Institut für Biochemie, Martinsried, Germany, and #Laboratoire de Chimie-Physique des Macromolécules aux Interfaces, Université Libre de Bruxelles, Brussels, Belgium

ABSTRACT Oriented multilamellar systems containing phospholipids and peptides have been formed on a germanium internal reflection element. Attenuated total reflection infrared spectra have been recorded and the linear dichroism of peptide amide I and amide II bands measured. Using peptides for which the orientation had been previously studied under similar experimental conditions by ^{15}N solid-state nuclear magnetic resonance spectroscopy, important conclusions were drawn on the approach to be used to derive secondary structure orientation in a membrane from dichroic ratios. In particular, it is shown that the influence of the film thickness and refractive index on the orientation determination can be evaluated from the value of R^{ATRiso}, i.e., the dichroic ratio of a dipole oriented at the magic angle or with isotropic mobility. A series of peptides was used to test the validity of our suggestions on various helix orientations in the membrane. These include magainin 2 and hydrophobic (hΦ20) model peptides, the transmembrane segment of glycophorin (GLY), and LAH_4, a designed peptide antibiotic that changes between a transmembrane and an in-plane orientation in a pH-dependent manner.

INTRODUCTION

Polarized attenuated total internal reflection infrared spectroscopy is presently one of the best tools available to obtain information on the orientation of peptides interacting with membranes. The method is simple (oriented multilayers systems are easily obtained by drying a membrane suspension on the internal reflection element), it is sensitive (less than 1 μg of peptide is required to form a single monolayer) and it does not require specific labeling (although specific labeling with ^{13}C allows the study of selected residues). Orientational order parameters are derived from the dichroic ratio of the amide I or amide II bands. The dichroic ratio is the ratio of the integrated absorption for parallel versus perpendicular polarized incident light. How accurately the orientation of peptide secondary structure is described by polarized ATR-FTIR spectroscopy is still a matter of debate as only a few peptides have been investigated under the same experimental conditions by both polarized ATR-FTIR and another technique that is able to determine their orientation with respect to the lipid bilayer. Furthermore, among those are several homopolymers that exhibit notable differences in their IR spectra when compared with polypeptides composed of a wider variety of amino acid residues.

To compute the peptide orientation with respect to the lipid membrane from experimental dichroic ratios, the knowledge of a number of parameters is necessary. These include the refractive index of the peptide in the absorbance band, the orientational distribution function of the transition dipole with respect to the secondary structure main symmetry axis, and the mosaic spread of the lipid membrane with respect to the internal reflection element, just to quote the poorly characterized ones. Moreover, the computation also depends on the model used to describe the system. In thin films (much thinner than the wavelength) the field is usually considered to be constant over the film thickness, whereas in thick films the evanescent field does not penetrate the whole depth of the sample. Intermediate thickness is usually not considered because of the difficulty to accurately control this parameter.

It is the goal of the present communication to experimentally determine the dichroic ratios for some peptides with well characterized orientation. Several peptides have, therefore, been reconstituted into lipid bilayers that were dried onto germanium internal reflection crystals and investigated by ATR-FTIR spectroscopy. The conformations of these peptides are predominantly α-helical in membrane environments as determined previously by multidimensional solution NMR or circular dichroism spectroscopies. In addition, the orientation of all except one has been investigated by ^{15}N solid-state NMR spectroscopy in uniaxially oriented bilayer systems (Bechinger et al., 1996). The experimental data from these peptides, therefore, provide the information necessary for the calibration of some model-dependent parameters used to quantitatively describe the orientation-dependent FTIR dichroism. Our approach also allows for a direct comparison of both techniques.

Received for publication 9 July 1998 and in final form 25 September 1998.

Address reprint requests to Dr. E. Goormaghtigh, Free University of Brussels, Campus Plaine CP 206/2, B1050 Brussels, Belgium. Tel.: 32-2 6505386; Fax: 32-2 6505113; E-mail: egoor@ulb.ac.be.

Abbreviations: FTIR, Fourier transform infrared; ATR, attenuated total reflection; IRE, internal reflection element; FWHH, full width at half-height; NMR, nuclear magnetic resonance; R^{ATR}, dichroic ratio; R^{ATRiso}, dichroic ratio for a dipole isotropically oriented; MALDI, matrix-assisted laser desorption ionization; HPLC, high-performance liquid chromatography; DOPC, 1,2-dioleoyl-*sn*-glycero-3-phosphocholine; DMPC, 1,2-dimyristoyl-*sn*-glycero-3-phosphocholine; $DLPEM_2$, 1,2-dilauroyl-*sn*-glycero-3-phospho-*N*,*N*-dimethylethanolamine; DMPG, 1,2-dimyristoyl-*sn*-glycero-3-phosphoglycerol; DPPG, 1,2-dipalmitoyl-*sn*-glycero-3-phosphocholine; POPC, 1-palmitoyl-2-oleoyl-*sn*-glycero-3-phosphocholine; MCT, mercury cadmium telluride; TFE, trifluoroethanol; $\Delta\sigma_{1/2}$, spectral line width at half-height (in ppm).

0006-3495/99/01/552/12 $2.00

One of the peptides investigated is magainin 2, a 23-residue immunogenic peptide found in the skin and intestines of frogs. The family of magainins has been shown to exhibit broad-spectrum antibiotic, fungicidal, virocidal, and tumorcidal activity. Related polypeptides have also been found in other amphibians, insects, or mammals (reviewed in Boman, 1991; Bechinger, 1997). Although magainins are well water soluble, they strongly interact with lipid membranes where they exhibit membrane-disruptive and channel-like activity. The interaction of these peptides with isolated mitochondria, lysosomal or spermatocoal membranes results in the decoupling of the respiratory chain from the transmembrane ionic gradients. Solution and solid-state NMR as well as a large range of optical spectroscopies all indicate that magainins exhibit a random coil conformation in aqueous solution but form amphipathic α-helical structures when associated with micelles or phospholipid membranes (Bechinger, 1997).

The LAH_4 peptide also forms an amphipathic helical structure. The hydrophobic face, however, covers a larger surface area. This peptide has been designed to change its orientation in the membrane in a pH-dependent manner (Bechinger, 1996), which allows the evaluation of the hydrophobic, polar, and electrostatic contributions that determine the orientation of membrane polypeptides. The histidines exhibit pK values between 5.4 and 6.0, and the electrostatic contributions during membrane insertion are, therefore, strongly dependent on pH.

Other examples of hydrophobic peptides that are predicted to cross the membrane are hΦ20, a peptide consisting of 20 alternating alanine and leucine residues and two flanking lysines at each terminus. These positively charged residues help to keep the peptide soluble, and they also act as interfacial anchors. The last peptide that will be presented in this paper is a derivative of the hydrophobic anchor of glycophorin. This sequence has been shown to form dimers in membrane-like environments through interactions along its hydrophobic surface (Lemmon et al., 1992). Although two residues have been exchanged to simplify the chemical synthesis of this hydrophobic sequence, care has been taken to keep the dimerization motive intact.

MATERIALS AND METHODS

Infrared spectroscopy

Attenuated total reflection infrared (ATR-FTIR) spectra were recorded on a Bruker IFS 55 infrared spectrophotometer equipped with a liquid-nitrogen-cooled MCT detector. The internal reflection element was a germanium ATR plate (50 × 20 × 2 mm) with an aperture angle of 45°. A total of 128 scans were accumulated for each spectrum. Spectra were recorded at a nominal resolution of 2 cm^{-1}. The spectrophotometer was continuously purged with air dried on a silica gel column (5 × 130 cm) at a flow rate of 7 L/min.

Peptides

Peptides with the following sequences were obtained by chemical peptide synthesis using Fmoc chemistry on ABI 431A and Millipore 9030 automatic peptide synthesizers: magainin 2 (GIGKF LHSAK KFGKA FVGEI MNS), LK21 (KKLLK LLKKL LKKLK KLLKK L), hΦ20 (KKLAL ALALA LALAL ALALA LAKK), and GLY (CEKEI TLIIF GVMAG VIGTI LLISY GIKEK C). Their purity and composition were controlled by reverse-phase HPLC and MALDI-mass spectrometry.

Preparation of the samples

Typically, 50–60 μg of peptide was dissolved in TFE/water 90/10 (v/v) at concentrations of 10–12 mg/ml. This solution was mixed with 500 μg of POPC in chloroform (Avanti Polar Lipids, Birmingham, AL) to obtain a final peptide concentration of approximately 10% (w/w). Oriented thin multilayer films were obtained by applying the solution onto one side of a germanium plate and drying it under a stream of N_2 (Fringeli and Günthard, 1981). Pure lipid bilayer preparations were subject to an identical treatment. To change pH, the preparation was overlaid twice with 600 μl of 66 mM phosphate buffer at the desired pH and incubated for 5 min. The buffer was carefully removed with a pipette before the film was dried under a stream of N_2.

Orientation of the secondary structures

The determination of molecular orientations by infrared ATR spectroscopy was previously reviewed by Fringeli and Günthard (1981) and Goormaghtigh and Ruysschaert (1990). Spectra were recorded with incident light, which is polarized parallel or perpendicular relative to the incidence plane. The dichroic spectrum is the difference between the spectra recorded with parallel and perpendicular polarizations. The perpendicular spectrum is multiplied by a factor of 1.34 before subtraction to take into account the differences in the relative power of the evanescent fields as will be discussed below. A larger absorbance for the parallel polarization (upward deviation on the dichroism spectrum) indicates a dipole oriented preferentially near the normal of the ATR plate. Conversely, a larger absorbance for the perpendicular polarization (downward deviation on the dichroism spectrum) indicates a dipole oriented approximately parallel to the ATR plate.

Fitting of the dichroic ratio, R^{ATR}, as a function of pH for LAH_4

^{15}N solid-state NMR spectroscopy indicates that LAH_4 changes between two extreme orientational states without intermediate orientations in a pH-dependent manner (Bechinger, 1996). The dichroic ratios of helices with orientations A and B are defined as

$$R_A^{ATR} = \frac{A_A^{\parallel}}{A_A^{\perp}} \quad R_B^{ATR} = \frac{A_B^{\parallel}}{A_B^{\perp}}, \tag{1}$$

where A stands for the integrated area of the absorption band considered. When both orientations coexist, the experimental dichroic ratio is given by

$$R^{ATR} = \frac{A_A^{\parallel} + A_B^{\parallel}}{A_A^{\perp} + A_B^{\perp}} \tag{2}$$

The dichroic ratio R^{ATR} does not depend linearly on the fraction of molecules in each orientation. The total, unpolarized contributions from helices A and B, however, must remain proportional to the fraction of helix with orientation A (x) or B ($1 - x$), respectively,

$$\frac{x}{1-x} = \frac{A_A^{\parallel} + 2A_A^{\perp}}{A_B^{\parallel} + 2A_B^{\perp}} \tag{3}$$

After introduction of Eqs. 1 and 2 into Eq. 3 and solving for x, one obtains

$$x = \frac{(R^{ATR} - R_B^{ATR})(R_A^{ATR} + 2)}{(R_B^{ATR} + 2)(R_A^{ATR} - R^{ATR}) - (R_A^{ATR} + 2)(R_B^{ATR} - R^{ATR})} \quad (4)$$

It is reasonable to assume that at extreme pH values all the helices have either the A or the B orientation, and the measured dichroic ratios correspond to the lowest (R_{min}^{ATR}) or the highest (R_{max}^{ATR}) possible values, respectively. After rearrangement of Eq. 4, the dichroic ratio dependence on pH is

$$R^{ATR} = \frac{f R_{min}^{ATR}(R_{max}^{ATR} + 2) + (1 - f)R_{max}^{ATR}(R_{min}^{ATR} + 2)}{f(R_{max}^{ATR} + 2) + (1 - f)(R_{min}^{ATR} + 2)}, \quad (5)$$

with the pH titration curve,

$$f = 1 - \left(\frac{10^{-x}}{10^{-pH_{50}}} \Big/ \left(1 + \frac{10^{-x}}{10^{-pH_{50}}}\right)\right) \quad (6)$$

or

$$f = \frac{10^{-x}}{10^{-pH_{50}}} \Big/ \left(1 + \frac{10^{-x}}{10^{-pH_{50}}}\right) \quad (7)$$

for the amide II or amide I signals, respectively. A nonlinear regression (Marquardt-Levenberg) was used to determine pK, R_{min}^{ATR}, and R_{max}^{ATR}.

RESULTS

Because the conformation and topology of the LAH_4 peptide have previously been characterized by multidimensional solution and proton-decoupled ^{15}N solid-state NMR spectroscopies (Bechinger, 1996), we started our ATR-FTIR investigations with this peptide. Fig. 1 shows the ATR-FTIR spectra of POPC-LAH_4 peptide for parallel and perpendicular orientations of the polarizer at pH 4.0 (solid line) and pH 9.0 (dashed line). The amide I signal is present as a narrow band (FWHH = 20 cm^{-1} at both pH values) centered around 1657 cm^{-1}, confirming the predominantly helical structure of the peptide at both pH values. The amide II band is present at 1546 cm^{-1}, in agreement with a helical conformation (for a review see Goormaghtigh et al., 1994a). The two other major bands in this region are assigned to POPC vibrations: 1739 cm^{-1} for the ester stretch vibrations ν(C═O) and 1468 cm^{-1} for the bending motion $\delta(CH_2)$. One additional band at 1588 cm^{-1}, only present at pH 9.0, is assigned to the deprotonated carboxylic end of the peptide $\nu_{as}(COO^-)$ and possibly also contains a contribution of the deprotonated histidine rings. A qualitative analysis of the orientations of the secondary structures is easily performed when the dichroic spectra are obtained by subtracting the parallel from perpendicular polarized spectra (Fig. 1, top). However, to take into account the differences in the relative power of the evanescent field, it is necessary to multiply the perpendicular spectrum by a factor $R^{ATRiso} = 1.34$, i.e., the dichroic ratio observed for an isotropically oriented sample, as will be discussed below in more detail. In the absence of any orientation, a straight line is expected. Positive deviations indicate a transition dipole oriented close to parallel to the membrane normal whereas negative deviations indicate a dipole alignment approximately in the membrane plane. In an α-helix, the amide I dipole is close to the helix long axis whereas the amide II dipole is roughly perpendicular to it (for a review see Goormaghtigh et al., 1994b). The dichroic spectra shown in Fig. 1 (top) demonstrate well defined orientations of LAH_4 at both pH values. At low pH, amide I dichroism is pointing downward and amide II dichroism is pointing upward, indicating an orientation of the helix axis close to the membrane plane. At high pH, the dichroisms observed are opposite in sign, indicating that the helix axis is close to perpendicular to the membrane plane. It must be noted that the lipid ν(C═O) dichroism is resolved in at least two components at 1748 and 1729 cm^{-1}, in agreement with band narrowing results obtained on DOPC (Siminovitch et al., 1987). The $\delta(CH_2)$ signal shows a negative dichroism at 1468 cm^{-1}. As this dipole is oriented perpendicular to the acyl chain long axis (Fringeli and Günthard 1981), this

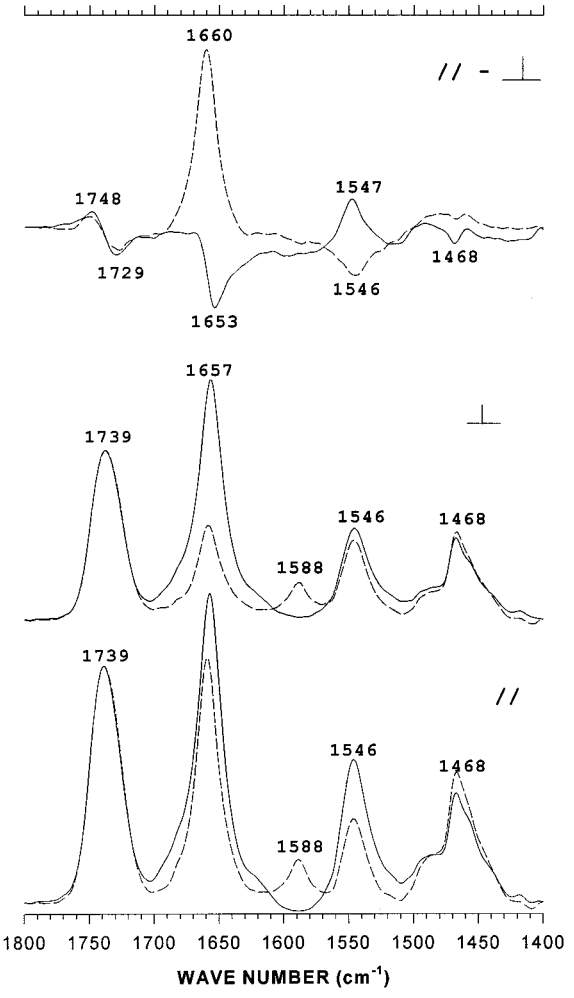

FIGURE 1 ATR-FTIR spectra of POPC-LAH_4 membranes for parallel and perpendicular orientations of the polarizer at pH 4.0 (———) and pH 9.0 (- - -). Dichroic spectra (*top*) were obtained as ∥ minus ⊥ spectra after multiplication of the ⊥ spectra by 1.34 (see text). All spectra are presented on the same scale but the dichroic spectra whose intensity has been doubled.

indicates the expected orientation of the lipid acyl chain parallel to the membrane normal.

The evolution of R^{ATR} as a function of pH is reported in Fig. 2. Around pH 6.5 a well defined transition in R^{ATR} for the amide I and amide II curves indicates a reorientation of the LAH_4 helix. The lipid ν(C═O) remains unchanged. Two separated signal intensities observed in ^{15}N solid-state NMR spectroscopy of oriented membrane samples demonstrate that at intermediate pH exchange of LAH_4 between these orientations is slow when compared with the time scale of ^{15}N chemical shift interaction (10^{-4} s). The midpoint of transition, pH_{50}, as well as minimal and maximal values of R^{ATR} have, therefore, been obtained from the pH-dependent dichroic ratios using a two-stage model (see Materials and Methods). The midpoint of transition of the amide I dichroism occurs at $pH_{50} = 6.54$. The maximal and minimal values of the dichroic ratio are $R^{ATR}_{max} = 2.83$ and $R^{ATR}_{min} = 1.29$. For the amide II signal, the curve fitting yields $pH_{50} = 6.46$, $R^{ATR}_{max} = 1.50$, and $R^{ATR}_{min} = 1.04$. The good agreement for the pH_{50} values measured for the amide I and amide II signals is obtained only when the pH curve is expressed according to Eq. 5, which takes into account both the dependence of orientation on pH and the nonlinear dependence of R^{ATR} on the orientation. The pH_{50} value obtained from the ATR-FTIR experiments also agrees with the ^{15}N solid-state NMR data, which indicate that the transmembrane and in-plane orientations are equally populated at $pH_{50} = 6.1 \pm 0.2$ (Bechinger, 1996). The maximal and minimal values of R^{ATR} for both amide signals depend on the optical properties of the sample as well as the dipole orientation of the amide I and II functional groups, respectively, as will be discussed later.

Other membrane peptides interacting with the lipid bilayer in a well defined orientation can help refine our knowledge on the minimal and maximal possible values of dichroic ratios R^{ATR} that can be reached. A series of peptides characterized by an α-helical structure oriented either parallel or perpendicular to the membrane surface has been tested. Both GLY and hΦ20 display a sharp amide I band (FWHH = 24 and 16 cm^{-1}, respectively) located at 1658 and 1660 cm^{-1}, respectively, confirming a helical structure of these peptides (Figs. 3 and 4). A positive dichroism in the amide I region and a negative dichroism in the amide II region indicate a transmembrane orientation of the helices. When the GLY-containing lipid film is incubated at room

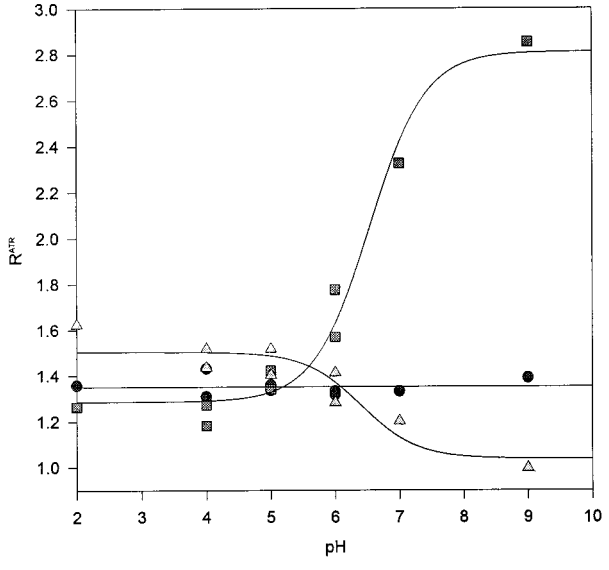

FIGURE 2 Evolution of the dichroic ratio of amide I (*squares*), amide II (*triangles*) and lipid ν(C═O) (*circles*) as a function of pH. For amide I, pH_{50} was found to be 6.54 from curve-fitting analysis (see Materials and Methods) $R^{ATR}_{max} = 2.82$ and $R^{ATR}_{min} = 1.29$. For amide II, the curve fitting yields pK = 6.46, $R_{max} = 1.50$, and $R_{min} = 1.04$. For the lipid ν(C═O), the slope of the linear regression is close to 0 (-7.3×10^{-6}) and the intercept is 1.34.

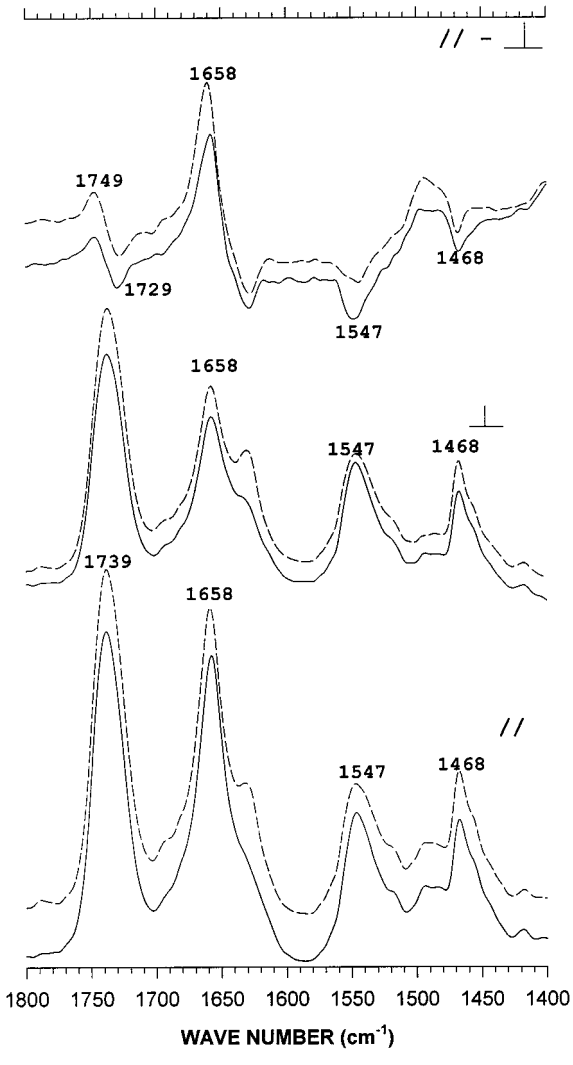

FIGURE 3 ATR-FTIR spectra of GLY peptide for parallel and perpendicular orientations of the polarizer. Spectra were recorded immediately after preparation (———) or after incubation overnight on the germanium crystal (- - -). Dichroic spectra (*top*) were obtained as ∥ minus ⊥ spectra after multiplication of the ⊥ spectra by 1.34 (see text). All spectra are presented on the same scale but the dichroic spectra whose intensity has been doubled.

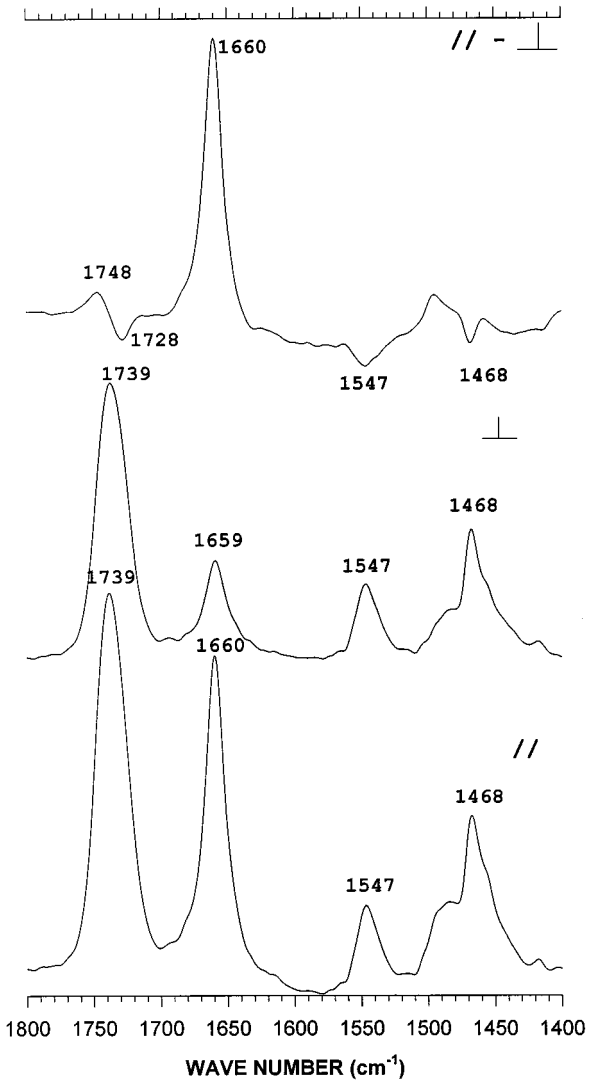

FIGURE 4 ATR-FTIR spectra of hΦ20 peptide for parallel and perpendicular orientations of the polarizer. The dichroic spectrum (*top*) was obtained as ∥ minus 1.34 × ⊥ spectra (see text). All spectra are presented on the same scale but the dichroic spectrum whose intensity has been multiplied by 1.5.

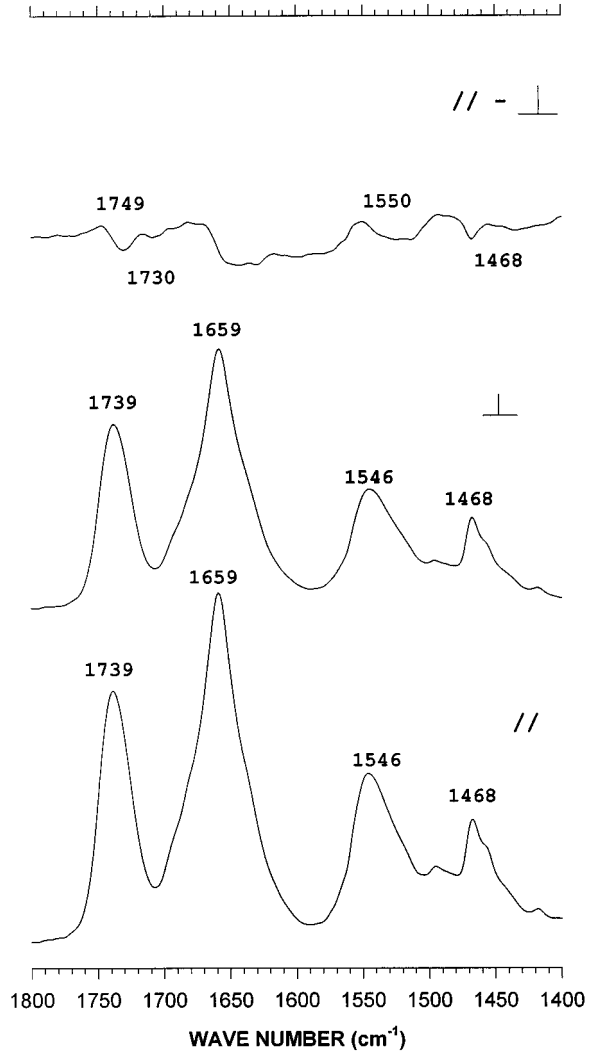

FIGURE 5 ATR-FTIR spectra of magainin 2 for parallel and perpendicular orientations of the polarizer. Dichroic spectra (*top*) were obtained as ∥ minus ⊥ spectra after multiplication of the ⊥ spectra by 1.34 (see text). All spectra are presented on the same scale but the dichroic spectrum whose intensity has been expanded twofold.

temperature overnight, a shoulder appears at 1628 cm^{-1} (Fig. 3), indicating a structural rearrangement, possibly due to the formation of β-sheet conformations in a fraction of the peptide. This β-sheet formation may be related to previous observations that the transmembrane proteolytic fragment of glycophorin A from erythrocyte membranes also displays a β-sheet component in its infrared spectrum (Challou et al., 1994). The amide I band of magainin 2 is located at 1659 cm^{-1} and exhibits a negative dichroism, indicating an in-plane helical structure (Fig. 5). This band, however, is relatively broad (FWHH = 33 cm^{-1}), which implies a larger conformational or orientational disorder, e.g., due to more scattering of the φ and ψ angles within the helical structure.

More quantitative information on the orientations of the peptides is contained in the dichroic ratio R^{ATR}. Values of R^{ATR} for amide I and amide II are reported in Table I for the different peptides studied so far. The lipid band dichroic ratios recorded in the same series of samples (not shown) are not significantly modified by the presence of the peptides: $\nu_{as}(CH_3)$ at 2559 cm^{-1}, 1.94 ± 0.30; $\nu_{as}(CH_2)$ at 2915 cm^{-1}, 1.22 ± 0.06; $\nu_{as}(CH_2)$ at 2875 cm^{-1}, 1.12 ± 0.06;

TABLE 1 Dichroic ratios of the amide I and II bands for the different peptides

	Amide I	Amide II
LAH_4, extrapolated, high pH	2.83	1.04
hΦ20	2.66	1.06
LAH_4, pH 7.0	2.30	1.20
GLY	1.60	1.10
LAH_4, extrapolated, low pH	1.29	1.50
Magainin 2	1.21	1.34

ν(C═O) at 1740 cm^{-1}, 1.34 ± 0.008; and $\delta(CH_2)$ at 1468 cm^{-1}, 1.11 ± 0.07 (average of 58 experiments on POPC in the absence or in the presence of the peptides, with standard deviations reported).

DISCUSSION

Frequency of amide I dichroism

The ATR-FTIR spectra of LAH_4 exhibit amide I maxima at 1657 cm^{-1} and identical FWHH at both low and high pH, suggesting the same helix geometry in both orientations (Fig. 1). Both spectral parameters are very sensitive to helix stability as reviewed elsewhere (Goormaghtigh et al., 1994b). The dichroism spectra, however, show distinct maxima at 1660 cm^{-1} for the transmembrane orientation and at 1653 cm^{-1} for the orientation of the helix parallel to the membrane surface. The increased frequency of the dichroism spectrum of transmembrane helices has been systematically observed before for membrane proteins (Bazzi and Woody, 1985; Goormaghtigh et al., 1991a,b; Rothschild and Clark, 1979a,b; and reviewed in Goormaghtigh et al., 1994b). It has, therefore, been suggested that transmembrane helices are characterized by a higher frequency when compared with helices in globular parts of the protein. The identical helix geometry found in the present experiments, however, supports the alternative hypothesis that the splitting of the parallel and perpendicular components of the amide I resonance are revealed in dichroism spectra (Earnest et al., 1990; Rath et al., 1991; Reisdorf and Krimm, 1995).

Quantitative interpretation of dichroic ratios

As developed elsewhere for the specific case of ATR (Goormaghtigh and Ruysschaert, 1990), the dichroic ratio R^{ATR} is related to an orientational order parameter S by

$$R^{ATR} = \frac{E_x^2}{E_y^2} + \frac{E_z^2}{E_y^2}\left(1 + \frac{3S}{1-S}\right), \tag{8}$$

where E_x^2, E_y^2, and E_z^2 are the time-averaged square electric field amplitudes of the evanescent wave in the film at the IRE/film interface. This equation supposes a uniaxial symmetry. This assumption is not valid for the protein β-sheet structure (Marsh, 1997) and for some phospholipids in the subgel phase (Nagle, 1993). The parameters necessary to compute the relationship between R^{ATR} and S are described in Appendix 1. The measured order parameter S, denoted below $S_{experimental}$, obtained from R^{ATR} through Eq. 8 can be generally expressed as a set of nested, uniaxial symmetric distributions (Rothschild and Clark, 1979b):

$$S_{experimental} = S_{membrane} S_{helix} S_{dipole}, \tag{9}$$

where $S_{membrane}$ describes the distribution function of the lipid membrane patches (smallest planar membrane unit) with respect to the internal reflection element; S_{helix}, the orientation of the helices within the membrane plane; and S_{dipole}, the dipole orientation of either amide I or amide II with respect to the helix long axis. S_{helix} can be further decomposed into an order function $S_{helix\ order}$ and a delta function, $S_{helix\ angle}$, describing the mean angle of the helix with respect to a membrane normal:

$$S_{helix} = S_{helix\ angle} S_{helix\ order} \tag{10}$$

This latest decomposition is artificial but useful for the reasoning below. Using Eq. 9 and 10, $S_{helix\ angle}$ can now be evaluated from $S_{experimental}$, and the helix mean tilt angle θ with respect to the membrane normal is calculated using the relation

$$S_{helix\ angle} = (3\cos^2\theta - 1)/2 \tag{11}$$

To obtain the helix orientation, i.e., $S_{helix\ angle}$, a number of problems must be dealt with. The first problem encountered is the evaluation of the different order parameters mentioned in Eqs. 9 and 10. First, the ordering of the membrane on the ATR crystal is usually quite good, and measurements performed elsewhere indicate that $S_{membrane}$ is close to 1 (Rothschild et al., 1980; Zhang et al., 1995). Second, the orientation of the amide I and amide II dipoles with respect to the helix axis remains difficult to assess. In view of the rather large uncertainty on S_{dipole}, its value will be discussed below in more detail with respect to the experimental data obtained here. Third, $S_{helix\ order}$ cannot be evaluated independently. Limiting values of $S_{helix\ angle}$, however, can be derived under the assumption of perfect helix order ($S_{helix\ order} = 1$) using Eq. 11. Deviations from this approximation, i.e., the presence of helix disorder as well as the presence of orientational disorder in the membrane stack would result in larger positive $S_{helix\ angle}$ values for transmembrane orientations or in larger negative values for orientations of the helix long axis closer to the membrane plane. In turn, when compared with the estimate based on perfect order hypothesis, the helix long axis mean tilt will be closer to the membrane normal in the case of transmembrane helices and closer to the membrane plane in case of helix orientations approximately parallel to the membrane surface. With these restrictions in mind, $S_{membrane}$ and $S_{helix\ order} = 1$ can be used to yield useful information.

In addition, the determination of $S_{experimental}$ from the measured value of R^{ATR} (Eq. 8) involves prior knowledge of a number of parameters to compute E_x, E_y, and E_z, including the refractive indices of the ATR crystal (n_1), the peptide film in the absorbance band (n_2), and the outside medium (n_3) (see Appendix 1). The electric fields also depends on the model representing the experimental system, i.e., thick film, thin film, or intermediate thickness of the film. For each new sample the IR spectroscopist faces the question of the validity of the model and of the parameters therein to derive $S_{experimental}$ from R^{ATR}. Checking the validity of the model and values for the refractive indices requires the complete description of $S_{membrane}$, S_{dipole}, $S_{helix\ angle}$, and $S_{helix\ order}$. Obtaining such a complete characterization is quite

unlikely in lipid-protein multilamellar films. On the other hand, we suggest here that R^{ATRiso}, i.e., the dichroic ratio for an isotropic distribution of the dipoles, can be measured and used to overcome this problem. Equation 8 becomes

$$R^{\mathrm{ATRiso}} = \frac{E_x^2 + E_z^2}{E_y^2} \tag{12}$$

As only E_z depends significantly on the various experimental parameters, we shall see that E_z is best obtained from R^{ATRiso}. In practice, finding a band that exhibits the isotropic value R^{ATRiso} is not a trivial matter as all the molecules composing the film are oriented with respect to the germanium interface, including water. We suggest, however, that the lipid ν(C═O) band exhibits a transition that is oriented close to the magic angle (54.7°). The rationale behind this hypothesis is found in the dynamic structure of phosphatidylcholine as determined by static ^{13}C solid-state NMR as well as ^{1}H solution NMR spectroscopies. To account for the small anisotropy of the *sn*-2 carbonyl ^{13}C solid-state NMR signals of phospholipids in liquid crystalline bilayers the orientation of the unique axis of the axially symmetric ^{13}C carbonyl tensor has been suggested to be oriented close to the magic angle relative to the symmetry axis of molecular motion (Wittebord et al., 1981; Braach-Maksvytis and Cornell, 1988; Smith et al., 1992). By comparison with model compounds the unique axis of the ^{13}C carbonyl tensor has been oriented approximately along the carbon-carbon vector of the CO—O—C bond within the sp2 plane (Smith et al., 1992). This orientation roughly coincides with the infrared CO—O single bond stretch vibration. The main axis of molecular motion is assumed to run parallel to the long axis of the phospholipid molecules. An alternative model takes into consideration that several conformations of the glycerol moiety have been observed in the x-ray diffraction structures of phospholipids (Hauser et al., 1988). To best explain the ^{2}H quadrupole splittings of phospholipids deuterated at the glycerol backbone when incorporated into lipid bilayers (Gally et al., 1981), the co-existence of several of these conformations and their fast exchange in liquid crystalline bilayers has been suggested. Exchange between at least four phospholipid conformations has been taken into consideration to analyze the J coupling constants measured during the NMR spectroscopic investigations of short-chain phospholipids in micellar solutions (Hauser et al., 1988). The relevant x-ray structures (DMPC1, DLPA, $DLPEM_2$, and DMPG1; cf. Hauser et al., 1988) indicate that the CO—O—C vector assumes a variety of orientations with respect to the molecular long axis (not shown). As some of these angles correspond to positive ^{13}C chemical shift anisotropies and others to negative values, fast conformational exchange results in averaging of the apparent anisotropies. In a similar manner the C═O direction of both fatty acyl chains assume values from close to parallel to close to perpendicular with respect to the molecular rotation axis when the same phospholipid x-ray structures are analyzed. On average, the C═O orientation is close to the magic angle with respect to the bilayer normal. Fast conformational exchange together with axial diffusion and additional molecular motions are, therefore, in agreement with an apparently isotropic signal of the ester C═O stretch vibration. IR spectroscopy with a time scale of $\sim 10^{-12}$ s could provide information on the different conformations whose contributions are averaged in NMR experiments. FTIR spectroscopy of isotope-labeled phosphatidylcholine (Lewis and McElhaney, 1992) indeed confirms a wider variety of conformations than previously described from the x-ray study of DMPC (Pearson and Pascher, 1979). Using polarized ATR-FTIR spectroscopy on thick DMPC and DPPC films, Hübner and Mantsch (1991) came to the conclusion that both *sn*-1 and *sn*-2 ester C═O are oriented at 62–66°($S = -0.18$ to -0.26) with respect to the membrane normal in both dry or fully hydrated oriented multilayers, with no significant change upon the temperature-induced phase transition. In the latter experiments the individual contributions of the *sn*-1 and *sn*-2 linkages were evaluated after labeling the *sn*-2 carbonyl with ^{13}C. A similar orientation of both carbonyls was determined.

Even though our knowledge about the orientation of the carbonyl groups should be further refined, we suggest that the dichroic ratio of the band at 1738 cm^{-1} provides a good estimate for R^{ATRiso}. The nonsignificant change in *sn*-1 or *sn*-2 dichroic ratios upon hydration or phase transition pointed out by Hübner and Mantsch (1991) increases our interest for this band. Computing the dichroic spectra by zeroing the integral ν(C═O) near 1738 cm^{-1} results in positive bands for peptide amide transitions for which the dipole is parallel to the acyl chain and negative intensities for transitions where the dipole is aligned perpendicular to the acyl chains (Table 1). In the present study a value of R^{ATRiso} of 1.34 ± 0.008 (standard error) is estimated, in good agreement with our previous investigations where similar amounts of materials were used (Goormaghtigh et al., 1991a,b (DMPC, $R^{\mathrm{ATR}} = 1.3$); de Jongh et al., 1995 (DOPC, DMPC, $R^{\mathrm{ATR}} = 1.3$–1.4); Vigneron et al., 1995 (asolectin, $R^{\mathrm{ATR}} = 1.41$); Raussens et al., 1997, 1998 (gastric tubulovesicles natural lipids, $R^{\mathrm{ATR}} = 1.55$)). This value is also consistent with the dichroism of other lipid bands as the transitions with dipoles perpendicular to the lipid acyl chains such as $\nu_{as}(CH_2)$, $\nu_s(CH_2)$, and $\delta(CH_2)$ all have dichroic ratios lower than R^{ATRiso}. Once the experimental value of R^{ATRiso} is established, it can be tested which of the models, thin, thick, or intermediate film, best relates $S_{\mathrm{experimental}}$ to R^{ATR}.

The present value of $R^{\mathrm{ATRiso}} = 1.34$ immediately excludes the thick-film hypothesis. Introducing the field values (Eqs. 15–17) in Eq. 12, R^{ATR} reduces to

$$R^{\mathrm{ATRiso}}_{\text{thick-film}} = \frac{2\sin^2\alpha - n_{21}^2}{\sin^2\alpha(1 + n_{21}^2) - n_{21}^2}, \tag{13}$$

which is always 2 for the incidence angle of $\alpha = 45°$ ($\sin^2\alpha = 0.5$) used throughout this work. This property is independent of the refractive indices. During the experiments de-

scribed in this paper, 50–100 μg of material was spread over an area of 5 cm^2, which results in a sample thickness of 0.1–0.2 μm (assuming a density of 1). This value is indeed much smaller than the wavelength (6.06 μm at 1650 cm^{-1}) but close to the penetration depth $d_p = 0.39$ μm at 1650 cm^{-1}. In cases where the sample is much thinner than the penetration depth (thin-film model) the field may be considered to be constant over the film thickness. In this hypothesis, R^{ATRiso} depends on the different refractive indices (Harrick, 1967). Introducing Eqs. 18–20 into Eq. 12 yields $R^{ATRiso} = 1.18$, just too small to explain the 1.34 value that has been determined experimentally. It is therefore necessary to take into account the film thickness. This is confirmed by the fact that the measured dichroic ratios, including R^{ATRiso}, depend on the amount of material used to make each film (see below). A rigorous treatment of the stratified medium formed by the IRE, the film, and the rarer medium has been developed by Hansen (1968, 1973) and used more recently by Axelsen and Citra (1997). For weak absorbing samples, a simple interpolation of the electric field amplitudes has been suggested by Fringeli (1992). For a film of thickness d,

$$E_k(d) = E_k^{thin} + (1 - e^{-d/d_p})(E_k^{thick} - E_k^{thin}), \qquad (14)$$

where k stands for the coordinate direction x, y, or z and thin and thick are the values calculated for the thin- and thick-film approximation; d_p is the penetration depth (Eq. 21). This equation is quite useful for biological samples for which the band of interest, including the amide I band in proteins can be considered to be weak absorbers. The effects of n_2, n_3, and the film thickness d become apparent from the dependence of E_x, E_y, E_z, and R^{ATRiso} on these parameters (Fig. 6). Fig. 6 indicates that only E_z and thereby R^{ATRiso} depend significantly on n_2, n_3, and d. We therefore suggest the use of the experimental value of R^{ATRiso} to evaluate E_z. This was done numerically by computing the film thickness using $n_1 = 4.0$ (germanium), $n_2 = 1.44$ (lipids), $n_3 = 1.0$ (air), and the experimental value of R^{ATRiso}. A value of $R^{ATRiso} = 1.34$ results in $d = 0.12$ μm, in close agreement with the estimation derived from the amount of membrane material used to prepare the film (see above). It must be stressed that this could be only an apparent thickness in case of a poor evaluation of n_2 and n_3. Doubts about the physical meaning of the refractive indices of films much thinner than the wavelength have been expressed recently (Axelsen and Citra, 1997). Furthermore, the value of the refractive index in the absorption bands is usually uncertain. We made here the arbitrary choice to adjust d such that E_z is correctly evaluated. As expected from Fig. 6, whatever the parameter we adjust, E_x and E_y are essentially unchanged and the value of E_z is determined to be in agreement with the experimental R^{ATRiso}. When n_2 or n_3 are adjusted instead of d, the same helix orientation within less than 1° is obtained (not shown).

To determine peptide orientations from FTIR data the value of S_{dipole} needs to be evaluated for the transition

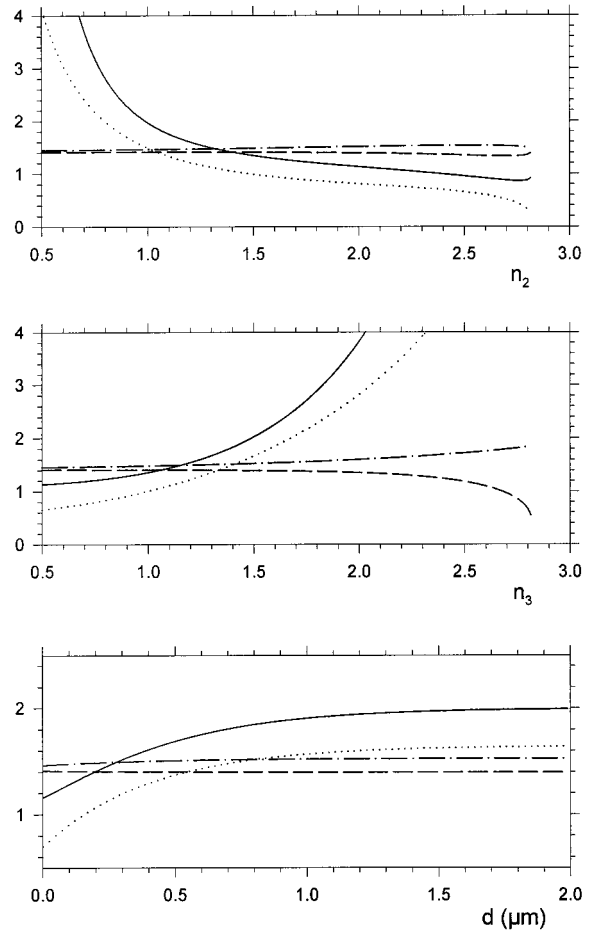

FIGURE 6 Dependence of E_x, E_y, E_z, and R^{ATRiso} on the film refractive index n_2 (*top*), on the external medium refractive index n_3 (*middle*), and on the film thickness d (*bottom*). Film thickness dependency was evaluated according to Eq. 14 (Fringeli, 1992). Incidence angle = 45°; $n_1 = 4.0$ (germanium). Where constant, $n_2 = 1.44$, $n_3 = 1.0$ (air), and $d = 0.12$ μm. ———, R^{ATRiso}; · · ·, E_z, — · —, E_y; - - -, E_x.

investigated. As reviewed previously (Goormaghtigh et al., 1994b), the angles between the amide I dipole and the helix main axis that are reported in the literature vary between 20° and 40°. This results in values for S_{dipole} between 0.82 and 0.38. Angles as large as 42–53° have been suggested when an $\alpha_{\|}$ structure was suspected (Draheim et al., 1991). The orientations reported for the amide II dipoles vary between 75° and 90° (S_{dipole} between −0.40 and −0.50). The dipole orientations are a function of the origin of the transition. Contributions to the potential energy of the amide I dipole are to 70–85% from ν(C═O), to 10–20% from ν(C—N), and to 10% from the C—CN deformation. It also contains some in-plane NH bending mainly responsible for the downshifts in the amide I frequency on N-deuteration (Krimm and Bandekar, 1986). The amide II potential energy derives from the in-plane N—H bending (40–60% of the potential energy), ν(C—N) (18–40%) and ν(C—C) (~10%). These factors and the resulting dipole orientation for amide I and amide II, therefore, depend on the exact

geometry of the helix. The maximal values observed for the transmembrane orientation of the helices for amide I and the minimal values for amide II observed in this work provide limits for S_{dipole}. Indeed, for $R^{ATR} = 2.82$ (Table 1), Eq. 8 yields an order parameter $S = S_{angle}S_{dipole} = 0.55$. If the helix is perfectly perpendicular to the membrane, $S_{angle} = 1$ and $S_{dipole} = 0.55$, corresponding to a maximal tilt of the dipole of 33.3° with respect to the helix axis. This value falls well within the range of the reported values for amide I in the case of α-helical conformations (for a review see Goormaghtigh et al., 1994b) and is close to the widely used value of 27° determined for bacteriorhodopsin (Rothschild and Clark, 1979b). It must be stressed here that the 33.3° value is an estimate for the maximal angle as both a tilt of the helix with respect to the membrane normal and/or some disordering of the membrane orientation would result in a lower calculated value. For instance, a helix tilt of 22° with respect to the membrane normal, a reasonable assumption that is in agreement with the experimentally determined static ^{15}N solid-state NMR chemical shift values in uniaxially oriented samples (see below), results in an angle between the dipole and the helix axis of 27°. Following the same reasoning the value of $R^{ATR} = 1.04$ (Table 1) for amide II implies a minimal tilt of the amide II dipole at 69° with respect to the helix axis.

To test the approach proposed above, which corrects for film thickness variations, we recorded ATR-FTIR spectra of POPC-LAH_4 peptide at pH 7.0 at parallel and perpendicular settings of the polarizer, similar to the experimental set-up described in Fig. 1. In this experiment, however, the film thickness was varied. Between 5 and 175 μg of material was spread over the approximate area of 5 cm^2. The evolution of the dichroic ratios for amide I, amide II, and lipid ν(C=O) as a function of the film weight is reported in Fig. 7 (bottom). As the amount of material is increased from 5 to 175 μg, R^{ATR} for amide I (pH 7.0) increases from 1.14 to 2.54 and for amide II (pH 5.0) from 0.92 to 2.08. In contrast, the amide II (pH 7.0) dichroic fatio decreases from 1.28 to 1.15 (not shown). With increasing film thickness, the lipid $\nu_s(CH_2)$ decreases from 1.15 to 1.05 and R^{ATR} for the lipid ν(C=O) increases from 1.17 to 1.41. At this point, two important features can be observed. First, for 5 μg, the lipid ν(C=O) has a dichroic ratio of 1.17, i.e., very close to the value of 1.18 obtained for a random distribution of the transition dipoles assuming the thin-film hypothesis. Second, as the film gets thinner, the accuracy of the experiment decreases and makes it more difficult to distinguish the various possible orientations whose characteristic dichroic ratios get closer. The bottom part of Fig. 7 also demonstrates that to deduce structural information from dichroic ratios of the film, thickness needs to be taken into consideration.

The values of R^{ATRiso} measured for the lipid ν(C=O) band shown in Fig. 7 (bottom) were used to compute the film thickness d (Fig. 7, middle) assuming an average orientation of the ester C=O bond close to the magic angle as suggested earlier. The calculated film dimensions are close to the expected ones on the basis of the amount of materials deposited on the germanium crystal. The maximal possible tilt for the amide I and amide II dipoles are subsequently calculated (Fig. 7, top) using the film thickness reported in Fig. 7 (middle). Clearly, even though the R^{ATR} variation is large (Fig. 7, bottom), at concentrations >10 μg, correction for the film thickness results in a consistent maximum 39 ± 2° tilt of the helix dipole with respect to the membrane normal (Eq. 8). The same behavior is seen in Fig. 7 for the amide II dipole. Deviation from this behavior occurs below 10 μg, i.e., for average film thickness smaller than 20 nm.

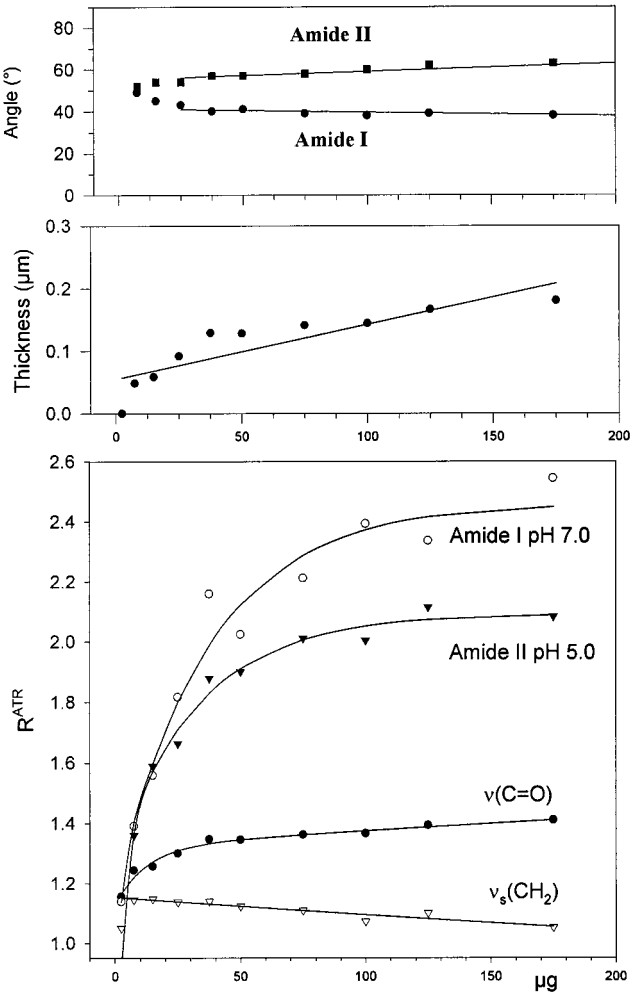

FIGURE 7 (*Bottom*) The dichroic ratios measured on a POPC-LAH_4 peptide film for amide I, amide II, and lipid ν(C=O) are shown as a function of the amount of material used to prepare the film. The film area is ~5 cm^2. (*Middle*) Film thickness, which has been calculated from R^{ATR} value measured for the lipid ν(C=O) using Eq. 14. (*Top*) Maximum tilt of the dipole of amide I and amide II transition with respect to the helix axis obtained when considering $S_{membrane} = 1$, $S_{helix\ angle} = 1$, and $S_{helix\ order} = 1$. Angles plotted are computed from the value of S_{dipole} obtained from Eq. 9 as $\arccos((2\ S_{dipole} + 1)/3)^{1/2}$.

Until now we have assumed that the peptide is fully α-helical. The presence of two to three unordered residues, however, has been suggested to occur at the termini of

helical structures (Dousseau and Pézolet, 1990; Kalnin et al. 1990). The presence of ~20% unordered residues introduces the following changes into the previous analysis (Raussens et al., 1997). According to the equations presented in Appendix 2 and considering an 80% helix content, R^{α} increases from 2.83 to 3.19, implying a maximal tilt of 32° for the helix amide I dipole. For amide II, R^{α} decreases from 1.04 to 1.00, implying a minimal tilt of the amide II dipole of 72°. These values are very close to the previous ones, indicating that the disorder introduced by the helix end does not significantly affect our conclusions.

The use of other peptides with marked orientations confirms the more general validity of these dipole orientations with respect to the helical structure. The hΦ20 peptide dichroism (Table 1) yields a maximal dipole tilt that is within 1° of the values discussed above. As pointed out by Reisdorf and Krimm (1995), the ratio of the amide I/amide II dichroism is not necessarily a constant as exemplified by GLY for which the amide II dichroism is close to the ones measured for hΦ20 or LAH_4, whereas the amide I dichroism is much less marked (Table 1).

Magainin exhibits the lowest negative dichroism for the amide I band. The peptide exhibits a preferred orientation approximately parallel to the surface. Among the peptides that have been used in this investigation, magainin 2 has been studied most extensively by the methods of solid-state NMR spectroscopy. Eight residues of the peptide have been labeled selectively with ^{15}N. Each of the peptides has been incorporated into uniaxially oriented phospholipid bilayers and studied in separate solid-state NMR experiments. One- and two-dimensional cross-polarization ^{15}N solid-state NMR spectroscopy indicates that the peptides form right-handed α-helical structures in lipid bilayers at least between residues 2 and 20 (Bechinger et al., 1993). These helices are stable on the time scale of the ^{15}N chemical shift anisotropy, and the measured ^{15}N chemical shifts indicate that this helix is oriented approximately parallel to the membrane surface. Although the chemical shift positions of the peaks are measured quite accurately ($<\pm 5$ ppm), the proton-decoupled ^{15}N resonances of early NMR spectra exhibit typical line width at half-height of ≤ 30 ppm. This value corresponds to $\leq 15\%$ of the static chemical shift anisotropy (~175 ppm). The line width is to a large extent due to orientational mosaic spread of these early samples ($d \approx 100$ μm) and is considerably reduced in more recent experiments where the thickness of membrane stacks was reduced (i.e., in conditions closer to those of the present study). Magainins labeled at the four consecutive positions between Ala-15 and Gly-18 have been investigated by multidimensional separated local-field NMR spectroscopy (Bechinger et al., 1993; Ramamoorthy et al., 1995). Among the low-energy structures tested, the measured ^{15}N chemical shifts and ^{1}H-^{15}N dipolar interactions agree only with a right-handed α-helix conformation. Among the eight residues labeled, the orientations of the Phe-16 and the Val-17 amides have been defined by the NMR parameters most accurately. Although the orientational restrictions are in perfect agreement with an energy-minimized right-handed α-helical structure, they do not overlap with the orientational restrictions of peptide bonds that form part of ideal α-helical conformations even though all possible helix orientations have been taken into consideration. The experimental values, however, are closest to angular restrictions obtained from an ideal helix oriented at 90° with respect to the bilayer normal. This indicates that magainin forms a nonideal helix conformation whose carboxyl-terminal part is oriented close to parallel to the membrane surface. These findings agree well with recent magainin structures in micellar solutions as determined by multidimensional NMR spectroscopy, which indicates a 16° bend in the α-helix around position 12 (Gesell et al., 1997; Bechinger et al., 1998a,b). The nonideal helix geometry makes an accurate definition of the average helix axis direction difficult. In addition, the assumption of a planar membrane surface seems only appropriate to first approximation in real samples. The comparison of FTIR to solid-state NMR measurements on oriented magainin-lipid samples underline that the orientations calculated from FTIR data are limits to the real average orientation of the helix with respect to the membrane as any kind of disorder introduced in the system through S_{membrane}, S_{helix}, or S_{dipole} will result in angles either closer to the membrane plane or to the membrane normal.

The approximate orientations of LAH_4 have been determined as a function of pH, using the ^{15}N solid-state chemical shift value as an indicator of transmembrane or in-plane orientations (Bechinger, 1996). The spectral intensities show that this peptide completely reorients from parallel to the surface into a transmembrane configuration when the pH is increased from 5 to 7. With the help of solid-state NMR experiments, the midpoint of transition has been determined to be $pH_{50} = 6.1$ (± 0.2) in good agreement with the FTIR titration shown in Fig. 2 ($pH_{50} = 6.5 \pm 0.2$). The pK values of the individual histidines have been measured by solution NMR spectroscopy and range between 5.4 and 6.0 in dodecylphosphocholine micelles. These values have been included into the analysis of electrostatic, polar, and hydrophobic energy contributions during the structural reorientation of the peptide (Bechinger, 1996, 1997).

The pH-dependent reorientation of LAH_4 has been observed by solid-state NMR as well as ATR-FTIR spectroscopies. Considering the differences in techniques and in sample conditions the experimentally determined midpoints of transitions agree considerably well. Whereas several thousand bilayers are oriented between pairs of glass plates at close to full hydration, the thin FTIR preparations are dried onto germanium crystals. A new membrane stack was prepared for each solid-state NMR measurement, and repeated incubation of the FTIR sample at different pH results in the observed reorientation. Whereas in ^{15}N solid-state NMR two different resonances have been integrated and compared (characteristic time scale 10^{-3}–10^{-4} s), a single averaged dichroic ratio is measured for the FTIR analysis (10^{-12}–10^{-14} s).

The ^{15}N chemical shift of the hΦ20 sequence indicates that this peptide orients parallel to the bilayer normal (±30°). The line width at half height of the ^{15}N resonance is ~30 ppm in samples that contain ≥100 μg of material per mm^2 ($d \approx 100$ μm). The glycophorin sequence has so far not been investigated by oriented solid-state NMR experiments although it has been used for distance measurements by magic-angle spinning solid-state NMR spectroscopy (Smith et al., 1994).

The model peptide hΦ20 exhibits narrow ^{15}N solid-state NMR resonances. The model character of this sequence with matching hydrophobic thickness, little variation in the amino acid side chains, and the clear-cut separation of hydrophobic and charged amino acids ensures that the sequence matches well with the amphipathic nature of the lipid bilayer. This sequence therefore exhibits a more homogeneous orientational distribution and disturbs the lipid bilayer orientation less than the natural sequences. The side chains of glycophorin and magainin exhibit additional interactions that cause deviations from ideal helical structures. Preliminary ^{31}P solid-state NMR results also suggest that these natural sequences cause severe distortions in the lipid bilayer planarity.

APPENDIX 1

According to Harrick (1967), for the thick-film hypothesis (film much thicker than the penetration depth of the evanescent wave, see below, Eq. 21), the field values are given by

$$E_{x,0} = \frac{2\cos\theta(\sin^2\theta - n_{21}^2)^{1/2}}{(1-n_{21}^2)^{1/2}[(1+n_{21}^2)\sin^2\theta - n_{21}^2]^{1/2}} \quad (15)$$

$$E_{z,0} = \frac{2\sin\theta\cos\theta}{(1-n_{21}^2)^{1/2}[(1+n_{21}^2)\sin^2\theta - n_{21}^2]^{1/2}} \quad (16)$$

$$E_{y,0} = \frac{2\cos\theta}{(1-n_{21}^2)^{1/2}} \quad (17)$$

and for the thin-film hypothesis (film much thinner than the penetration depth of the evanescent wave, see below, Eq. 21) by

$$E_{x,0} = \frac{2\cos\theta(\sin^2\theta - n_{31}^2)^{1/2}}{(1-n_{31}^2)^{1/2}[(1+n_{31}^2)\sin^2\theta - n_{31}^2]^{1/2}} \quad (18)$$

$$E_{z,0} = \frac{2n_{32}^2\sin\theta\cos\theta}{(1-n_{31}^2)^{1/2}[(1+n_{31}^2)\sin^2\theta - n_{31}^2]^{1/2}} \quad (19)$$

$$E_{y,0} = \frac{2\cos\theta}{(1-n_{31}^2)^{1/2}}, \quad (20)$$

where θ is the incidence angle, $n_{21} = n_2/n_1$, $n_{31} = n_3/n_1$, and $n_{32} = n_3/n_2$ with n_1, n_2, and n_3 the refractive indices of the internal reflection element, the sample, and the outer medium, respectively. The penetration depth is the distance from the germanium/film interface where the electric field amplitudes has decreased to 1/e (Harrick, 1967). It is given by

$$d_p = \frac{\lambda_1}{2\pi(\sin^2\theta - n_{21}^2)^{1/2}}, \quad (21)$$

where $\lambda_1 = \lambda/n_1$. S is defined as the projection of the orientational density distribution function $C(\Gamma)$ on the second Legendre polynomial. For uniaxial symmetry, it is computed as

$$S = \int_0^{\pi} \frac{3\cos^2\Gamma - 1}{2} C(\Gamma)\sin(\Gamma)d\Gamma, \quad (22)$$

where Γ refers to the angle of the considered distribution. Polarized infrared spectroscopy information is intrinsically limited to the second-order approximation of the distribution functions (Axelsen and Citra, 1997).

APPENDIX 2

In polarized spectra, the α-helix contribution to the amide band is

$$A_\alpha^{\parallel} = A^{\parallel} - A_u^{\parallel} \quad (23)$$

$$A_\alpha^{\perp} = A^{\perp} - A_u^{\perp}, \quad (24)$$

where the index u refers to the fraction of the polypeptide chain with no preferential orientation. By definition,

$$R^{\mathrm{ATRiso}} = A_u^{\parallel}/A_u^{\perp} \quad (25)$$

With x being the fraction of α-helix component in the protein, the α-helix dichroic ratio R^α is given by (Raussens et al., 1997)

$$R^\alpha = A_\alpha^{\parallel}/A_\alpha^{\perp} = \frac{R - \dfrac{R+2}{2R^{\mathrm{ATRiso}}+1}(1-x)}{1 - \dfrac{1}{R^{\mathrm{ATRiso}}}\dfrac{R+2}{2R^{\mathrm{ATRiso}}+1}(1-x)} \quad (26)$$

REFERENCES

Axelsen, P. H., and M. J. Citra. 1997. Orientational order determination by internal reflection infrared spectroscopy. *Prog. Biophys. Mol. Biol.* 66: 227–253.

Bazzi, M. D., and R. W. Woody. 1985. Oriented secondary structure in integral membrane proteins: circular dichroism and infrared spectroscopy of cytochrome c oxidase in multilamellar films. *Biophys. J.* 48: 957–966.

Bechinger, B. 1996. Towards membrane protein design: pH dependent topology of histidine-containing polypeptides. *J. Mol. Biol.* 263: 768–775.

Bechinger, B. 1997. Structure and functions of channel-forming polypeptides: magainins, cecropins, melittin and alamethicin. *J. Membr. Biol.* 157:197–211.

Bechinger, B., L. M. Gierasch, M. Montal, M. Zasloff, and S. J. Opella. 1996. Orientations of helical peptides in membrane bilayers by solid-state NMR spectroscopy. *Solid State Nuclear Magnetic Resonance* 7:185–192.

Bechinger, B., M. Zasloff, and S. J. Opella. 1993. Structure and orientation of the antibiotic peptide magainin in membranes by solid-state nuclear magnetic resonance spectroscopy. *Protein Sci.* 2:2077–2084.

Bechinger, B., Zasloff, M., and Opella, S. J. 1998a. Structure, orientation and dynamics of designed amphipathic helical peptides in membranes by multidimensional high-resolution and solid-state nuclear magnetic resonance spectroscopy. *Biophys. J.* In press.

Bechinger, B., Zasloff, M., and Opella, 1998b. S. J. Structure and dynamics of the antibiotic peptide PGLa in membranes by multidimensional solution and solid-state NMR spectroscopy. *Biophys. J.* 74:981–987.

Boman, H. G. 1991. Antibacterial peptides: key components needed in immunity. *Cell.* 65:205–207.

Braach-Maksvytis, V. L. B., and B. A. Cornell. 1988. Chemical shift anisotropies obtained from aligned egg yolk phosphatidylcholine by solid-state ^{13}C nuclear magnetic resonance. *Biophys. J.* 53:839–843.

Challou, N., E. Goormaghtigh, V. Cabiaux, K. Conrath, and J. M. Ruysschaert. 1994. Sequence and structure of the membrane-associated peptide of glycophorin A. *Biochemistry.* 33:6902–6910.

de Jongh, H., E. Goormaghtigh, and A. Killian. 1995. Analysis of circular dichroism spectra of oriented protein-lipid complexes: towards a general application. *Biochemistry.* 33:14521–14528.

Dousseau, F., and M. Pézolet. 1990. Determination of the secondary structure contents of proteins in aqueous solutions from their amide I and amide II infrared bands: comparison between classical and partial least-squares methods. *Biochemistry.* 29:8771–8779.

Draheim, J. E., N. J. Gibson, and J. Y. Cassim. 1991. Dramatic in situ conformational dynamics of the membrane protein bacteriorhodopsin. *Biophys. J.* 60:89–100.

Earnest, T. N., J. Herzfeld, and K. J. Rothschild. 1990. Polarized FTIR of bacteriorhodopsin: transmembrane α-helices are resistant to hydrogen-deuterium exchange. *Biophys. J.* 58:1539–1546.

Fringeli, U. P. 1992. *In situ* infrared attenuated total reflection (IR ATR) spectroscopy: a complementary analytical tool for drug design and drug delivery. *Chimia* 46:200–214.

Fringeli, U. P., and H. H. Günthard. 1981. Infrared membrane spectroscopy. *In* Membrane Spectroscopy. E. Grell, editor. Springer-Verlag, Berlin. 270–332.

Gally, H. U., G. Pluschke, P. Overath, and J. Seelig. 1981. Structure of *Escherichia coli* membranes: glycerol auxotrophs as a tool for the analysis of the phospholipid head-group region by deuterium magnetic resonance. *Biochemistry.* 20:1826–1831.

Gesell, J., M. Zasloff, and S. J. Opella. 1997. Two-dimensional ^{1}H NMR experiments show that the 23-residue magainin antibiotic peptide is an α-helix in dodecylphosphocholine micelles, sodium dodecylsulfate micelles, and trifluoroethanol/water solution. *J. Biomol. NMR* 9:127–135.

Goormaghtigh, E., V. Cabiaux, and J. M. Ruysschaert. 1994a. Determination of soluble and membrane protein structure by Fourier transform infrared spectroscopy III: secondary structures. *Subcell. Biochem.* 23: 405–450.

Goormaghtigh, E., V. Cabiaux, and J. M. Ruysschaert. 1994b. Determination of soluble and membrane protein structure by Fourier transform infrared spectroscopy. I. Assignments and model compounds. *Subcell. Biochem.* 23:329–362.

Goormaghtigh, E., J. De Meutter, V. Cabiaux, F. Szoka, and J. M. Ruysschaert. 1991a. Secondary structure and orientation of the amphipathic peptide GALA in lipid structures: an infrared spectroscopy approach. *Eur. J. Biochem.* 195:421–429.

Goormaghtigh, E., and J. M. Ruysschaert. 1990. Polarized attenuated total reflection spectroscopy as a tool to investigate the conformation and orientation of membrane components. *In* Molecular Description of Biological Membranes by Computer Aided Conformational Analysis, Vol. I. R. Brasseur, editor. CRC Press, Boca Raton, FL. 285–329.

Goormaghtigh E., L. Vigneron, M. Knibiehler, C. Lazdunski and J. M. Ruysschaert. 1991b. Secondary structure of the membrane-bound form of the pore-forming domain of colicin A: a FTIR-ATR study. *Eur. J. Biochem.* 202:1299–1305.

Harrick, N. J. 1967. Internal Reflection Spectroscopy. Interscience Publishers (John Wiley & Sons), New York.

Hauser, H., I. Pascher, and S. Sundell. 1988. Preferred conformation and dynamics of the glycerol backbone in phospholipids: an NMR and X-ray single-crystal analysis. *Biochemistry.* 27:9166–9174.

Hübner, W., and H. H. Mantsch. 1991. Orientation of specifically $^{13}C{=}O$ labeled phosphatidylcholine multilayers from polarized attenuated total reflection FT-IR spectroscopy. *Biophys. J.* 59:1261–1272.

Kalnin, N. N., I. A. Baikalov, and S. Y. Venyaminov. 1990. Quantitative IR spectrophotometry of peptide compounds in water (H_2O) solutions. III. Estimation of the protein secondary structure. *Biopolymers.* 30: 1273–1280.

Krimm, S., and J. Bandekar. 1986. Vibrational spectroscopy and conformation of peptides, polypeptides and proteins. *Adv. Protein Chem.* 38:181–364.

Lemmon, M. A., J. M. Flanagan, J. F. Hunt, B. D. Adair, B. J. Bormann, C. E. Dempsey, and D. M. Engelman. 1992. Glycophorin A dimerization is driven by specific interactions between transmembrane alpha-helices. *J. Biol. Chem.* 267:7683–7689.

Lewis R. N. A. H., and R. N. McElhaney. 1992. Structures of the subgel phases of n-saturated diacylphopshatidylcholine bilayers: FTIR spectroscopic studies of $^{13}C{=}O$ and ^{2}H labeled lipids. *Biophys. J.* 61:63–77.

Marsh, D. 1997. Dichroic ratios in polarized Fourier transform infrared nonaxial symmetry of β-sheet structures. *Biophys. J.* 72:2710–2718.

Nagle, J. F. 1993. Evidence of partial rotational order in gel phase DPPC. *Biophys. J.* 64:1110–1112.

Pearson, R. H., and I. Passcher. 1979. The molecular structure of lecithin dihydrate. *Nature (Lond.).* 281:499–501.

Ramamoorthy, A., F. M. Marassi, M. Zasloff, and S. J. Opella. 1995. Three-dimensional solid-state NMR spectroscopy of a peptide oriented in membrane bilayers. *J. Biomol. NMR.* 6:329–334.

Rath, P., O. Bouché, A. R. Merril, W. A. Cramer, and K. J. Rothschild. 1991. Fourier transform infrared evidence for a predominantly α-helical structure of the membrane bound channel forming COOH-terminal peptide of colicin E1. *Biophys. J.* 59:516–522.

Raussens, V., H. De Jongh, M. Pézolet, J. M. Ruysschaert, and E. Goormaghtigh. 1998. Secondary structure of the intact H^+,K^+-ATPase and its membrane embedded region: an attenuated total reflection infrared spectroscopy, circular dichroism and Raman spectroscopy study. *Eur. J. Biochem.* 252:261–267.

Raussens, V., J. M. Ruysschaert, and E. Goormaghtigh. 1997. Fourier transform infrared spectroscopy study of the secondary structure of the gastric H^+,K^+-ATPase and of its membrane-associated proteolytic peptides. *J. Biol. Chem.* 276:262–270.

Reisdorf, W. C., and S. Krimm. 1995. Infrared dichroism of amide I and amide II modes of $\alpha_|$- and $\alpha_\|$-helix segments in membrane proteins. *Biophys. J.* 69:271–273.

Rothschild, K. J., and N. A. Clark. 1979a. Anomalous amide I infrared absorption of purple membrane. *Science.* 204:311–312.

Rothschild, K. J., and N. A. Clark. 1979b. Polarized infrared spectroscopy of oriented purple membrane. *Biophys. J.* 5.25:473–488.

Rothschild, K. J., R. Sanches, T. L. Hsiao, and N. A. Clark. 1980. A spectroscopic study of rhodopsin α-helix orientation. *Biophys. J.* 31: 53–64.

Siminovitch, D. J., P. T. T. Wong, and H. H. Mantch. 1987. Effects of *cis* and *trans* unsaturation of the structure of phospholipids bilayers: a high-pressure infrared spectroscopy study. *Biochemistry.* 26:3277–3287.

Smith, S. O., R. Jonas, M. Braiman, and B. J. Bormann. 1994. Structure and orientation of the transmembrane domain of glycophorin A in lipid bilayers. *Biochemistry.* 33:6334–6341.

Smith, S. O., I. Kustanovich, S. Bhamidipati, A. Salmon, and J. A. Hamilton. 1992. Interfacial conformation of dipalmitoylglycerol and dipalmitoylphosphatidylcholine in phospholipid bilayers. *Biochemistry.* 31: 11660–11664.

Vigneron, L., J. M. Ruysschaert, and E. Goormaghtigh. 1995. Fourier transform infrared spectroscopy study of the secondary structure of the reconstituted *Neurospora crassa* plasma membrane H^+-ATPase and of its membrane-associated proteolytic peptides. *J. Biol. Chem.* 270: 17685–17696.

Wittebord, R. J., Schmidt, C. F., and Griffin, R. G. 1981. Solid-state carbon-13 nuclear magnetic resonance of the lecithin gel to liquid-crystalline phase transition. *Biochemistry.* 20:4223–4228.

Zhang, Y. P., R. N. Lewis, G. D. Henry, B. D. Sykes, R. S. Hodges, and R. N. McElhaney. 1995. Peptide models of helical hydrophobic transmembrane segments of membrane proteins. I. Studies of the conformation, intrabilayer orientation, and amide hydrogen exchangeability of Ac-K2-(LA)12-K2-amide. *Biochemistry.* 34:2348–2361.